Increased Brain Fatty Acid Uptake in Metabolic Syndrome

Anna Karmi,[1] Patricia Iozzo,[1,2] Antti Viljanen,[1] Jussi Hirvonen,[1] Barbara A. Fielding,[3] Kirsi Virtanen,[1] Vesa Oikonen,[1] Jukka Kemppainen,[4] Tapio Viljanen,[1] Letizia Guiducci,[1,2] Merja Haaparanta-Solin,[1] Kjell Någren,[5] Olof Solin,[1] and Pirjo Nuutila[1,6]

OBJECTIVE—To test whether brain fatty acid uptake is enhanced in obese subjects with metabolic syndrome (MS) and whether weight reduction modifies it.

RESEARCH DESIGN AND METHODS—We measured brain fatty acid uptake in a group of 23 patients with MS and 7 age-matched healthy control subjects during fasting conditions using positron emission tomography (PET) with [^{11}C]-palmitate and [^{18}F]fluoro-6-thia-heptadecanoic acid ([^{18}F]-FTHA). Sixteen MS subjects were restudied after 6 weeks of very low calorie diet intervention.

RESULTS—At baseline, brain global fatty acid uptake derived from [^{18}F]-FTHA was 50% higher in patients with MS compared with control subjects. The mean percentage increment was 130% in the white matter, 47% in the gray matter, and uniform across brain regions. In the MS group, the nonoxidized fraction measured using [^{11}C]-palmitate was 86% higher. Brain fatty acid uptake measured with [^{18}F]-FTHA-PET was associated with age, fasting serum insulin, and homeostasis model assessment (HOMA) index. Both total and nonoxidized fractions of fatty acid uptake were associated with BMI. Rapid weight reduction decreased brain fatty acid uptake by 17%.

CONCLUSIONS—To our knowledge, this is the first study on humans to observe enhanced brain fatty acid uptake in patients with MS. Both fatty acid uptake and accumulation appear to be increased in MS patients and reversed by weight reduction.
***Diabetes* 59:2171–2177, 2010**

Although the brain does not use free fatty acids (FFAs) as an energy source, recent evidence suggests that FFAs and, specifically, their intermediates could have a key role in the central control of energy balance regulation and feeding (1–5). Both brain FFA uptake and metabolism are currently insufficiently defined, whereas the importance of FFAs in the pathogenesis of metabolic syndrome (MS) is demonstrated widely in other organs (6,7). Animal studies have demonstrated that hypothalamic sensing of circulating fatty acids in general is believed to be important in controlling nutrient intake and, thus, energy balance. For example, Pocai et al. (5) showed that manipulation of central hypothalamic FFA metabolism normalizes energy and glucose homeostasis in overfed rats. These regulatory processes are difficult to address in humans in vivo, and most data in this regard have been demonstrated in small animals (1,4,5,8). More work is needed to clarify the mechanisms behind the complex hypothalamic regulatory circuitry that regulates energy expenditure and feeding behavior.

Positron emission tomography (PET) and other methods have been used to evaluate the fate of long-chain saturated fatty acid carbon-labeled-palmitate (9–12). PET provides a method for noninvasive, quantitative, and regional measurement of FFA uptake, thus making it ideal for studying metabolism in different tissues (13). The status of brain FFA metabolism in MS is currently unknown. Therefore, our aim was to use PET to examine possible difference in the brain FFA-uptake rates between MS patients and healthy individuals.

RESEARCH DESIGN AND METHODS

Subjects. Twenty-three subjects with MS (age 43 ± 7 years, BMI 33.6 ± 4.0 kg/m^2, 8 men and 15 women) and 7 age-matched healthy men (age 42 ± 11 years, BMI 26.8 ± 2.5 kg/m^2) (Table 1) were recruited, mostly from an occupational healthy service clinic. Healthy patients were nonobese and had normal oral glucose tolerance test results, whereas the 23 MS patients had MS according to the current International Diabetes Federation criteria (14) (Table 2). According to the criteria, a person defined as having MS must have central obesity, defined as increased waist circumference plus at least two other additional criteria (raised triglycerides/blood pressure/fasting glucose or reduced HDL). Subjects were told to use no alcohol during the study period. Smoking was an exclusion criterion. Only 1 of 23 subjects with MS used medication (ACE inhibitor for blood pressure). Written informed consents were obtained after explaining the purpose and potential risks of the study to the subjects. The study protocol was approved by the Ethics Committee of the Hospital District of Southwest Finland and conducted according to the principles of the declaration of Helsinki.

Study design. The study was designed to assess *1*) the differences between MS patients and healthy individuals at baseline, and *2*) the effect of a very low caloric diet (VLCD) in MS patients. Two PET studies were performed, first with [^{11}C]-palmitate, and thereafter with [^{18}F]fluoro-6-thia-heptadecanoic acid ([^{18}F]-FTHA), either during the same day or on separate days within 1 week. A subgroup of patients with MS (n = 16) were prescribed a VLCD. All daily meals were replaced by diet products for 6 weeks (Nutrifast, Leiras, Finland, 2.3 MJ (megajoule), 4.5 g fat, 59 g protein, and 72 g carbohydrate per day). After the diet there was a 1-week recovery period with an isocaloric diet to avoid catabolic state. The isocaloric diet was based on estimations of energy expenditure and was introduced by a physician. The assessments using PET were repeated. Magnetic resonance images were obtained for anatomical reference.

Production and nature of radiotracers. The production of [^{11}C]-palmitate (half-life 20.4 min) (15) and the production of [^{18}F]-FTHA (half-life 109 min): (16) are described elsewhere. The radiochemical purity of the final product

From the [1]Turku PET Centre, University of Turku and Turku University Hospital, Turku, Finland; the [2]PET Centre, Institute of Clinical Physiology, National Research Council, Pisa, Italy; the [3]Oxford Centre for Diabetes, Endocrinology, and Metabolism, University of Oxford, Churchill Hospital, Oxford, U.K.; the [4]Department of Clinical Physiology and Nuclear Medicine, University of Turku and Turku University Hospital, Turku, Finland; the [5]Department of Clinical Physiology and Nuclear Medicine, PET and Cyclotron Unit, Rigshospitalet, Copenhagen University, Copenhagen, Denmark; and the [6]Department of Medicine, University of Turku and Turku University Hospital, Turku, Finland.

Corresponding author: Pirjo Nuutila, pirjo.nuutila@utu.fi.

Received 30 January 2009 and accepted 14 June 2010. Published ahead of print at http://diabetes.diabetesjournals.org on 21 June 2010. DOI: 10.2337/db09-0138.

© 2010 by the American Diabetes Association. Readers may use this article as long as the work is properly cited, the use is educational and not for profit, and the work is not altered. See http://creativecommons.org/licenses/by-nc-nd/3.0/ for details.

The costs of publication of this article were defrayed in part by the payment of page charges. This article must therefore be hereby marked "advertisement" in accordance with 18 U.S.C. Section 1734 solely to indicate this fact.

TABLE 1
Baseline anthropometric and metabolic characteristics

	Metabolic syndrome	Healthy	*P* value
n (female/male)	23 (15/8)	7 (0/7)	
Age, years	43 ± 7	42 ± 11	NS
Weight, kg	98.7 ± 12.1	84.9 ± 8.6	0.009
BMI, kg/m^2	33.6 ± 4.0	26.8 ± 2.5	<0.0003
Fasting glucose, mg/dl	109.8 ± 12.6	97.2 ± 3.6	<0.02
OGTT glucose, 60 min, mg/dl	156.6 ± 54.0	176.4 ± 12.6	NS
OGTT glucose, 120 min, mg/dl	129.6 ± 52.2	100.8 ± 19.8	NS
Fasting insulin, mU/l	6.8 ± 2.6	3.9 ± 1.6	0.02
Total cholesterol, mg/dl	185.6 ± 34.8	170.1 ± 23.2	NS
HDL cholesterol, mg/dl	50.3 ± 11.6	50.3 ± 7.7	NS
Triglycerides, mg/dl	115.1 ± 53.1	88.6 ± 53.1	NS
LDL cholesterol, mg/dl	112.1 ± 34.8	100.5 ± 23.2	NS
HOMA index	1.8 ± 0.7	0.9 ± 0.4	0.02

Data are mean ± SD unless otherwise indicated. Fasting insulin values are from PET-scanning day. Homeostasis model assessment (HOMA) index calculated (fasting insulin × fasting glucose)/22.5. *P* values obtained from Student *t* test. NS, not significant.

was >98% for both tracers. [^{18}F]-FTHA ([^{18}F]fluoro-6-thia-heptadecanoic acid) is a long-chain FA analog that has a sulfur-substitution in the sixth carbon and a radioactive fluorine-18 label. [^{18}F]-FTHA which is taken up by tissues and subsequently either enters mitochondria or is incorporated into complex lipids (16). In mitochondria, [^{18}F]FTHA undergoes initial steps of β-oxidation and is thereafter trapped as further β-oxidation is blocked by its sulfur heteroatom (17). Because of these properties, [^{18}F]-FTHA provides optimal target-to-background signal in PET images.

In vivo validation of biodistribution of [^{18}F]-FTHA and [^{13}C]-palmitate in pig brain. To validate the biodistribution of both [^{18}F]-FTHA and [^{13}C]-palmitate in brain, we used data from in vivo pig [^{18}F]-FTHA biodistribution study (18), and completed the study by analyzing the biodistribution of stable [^{13}C]-palmitate from frozen brain samples obtained from the same animals. The study protocol and analysis of [^{18}F]-FTHA has been described in detail elsewhere (18), and the palmitate information is provided in an online appendix in an online appendix available at http://diabetes.diabetesjournals.org/cgi/content/full/db09-0138/DC1. The results are provided in Table 3. Roughly 62% from [^{13}C]-palmitate and 69% from [^{18}F]-FTHA was found in brain lipids. Most of the [^{13}C]-palmitate in brain lipids was found in phospholipids, and only trace amounts were found in triglycerides and fatty acids. [^{18}F]-FTHA was found mostly in triglycerides.

PET studies. Patients were scanned in the fasting state, and they refrained from drinks containing caffeine, smoking, and all medications for 12 h before the PET scan. Studies were performed in a supine position. Two catheters were inserted in the antecubital veins of different arms: one for saline infusion and tracer injection, and another for blood sampling. [^{11}C]-palmitate scan was performed before [^{18}F]-FTHA. [^{18}F]-FTHA scan was started after 7 half-lives of [^{11}C]-palmitate had occurred. The mean doses of injected [^{11}C]-palmitate and [^{18}F]-FTHA were 312 ± 148 MBq and 182 ± 17 MBq. With [^{11}C]-palmitate, dynamic brain scanning started immediately after injection (frames 8×15s, 2×30s, 2×120s, 1×180s, and 2×300s). Healthy individuals and MS patients not subscribed to VLCD were scanned with [^{18}F]-FTHA immediately after injection (frames 3×60s, 1×120s, 5×300s, 2×600s). For MS patients subscribed to VLCD, [^{18}F]-FTHA scanning started 70 min after injection and was static (600 s). During the scans, arterialized venous blood samples were drawn for the determination of plasma radioactivity (0, 15, 30, 45, 60, 75, 90, 105 s, and 2, 3, 4, 5, 10, 15, 20, 30, 40, 50 min for both [^{11}C]-palmitate and [^{18}F]-FTHA, and additional time points of 60, 70, 80, and 90 min for [^{18}F]-FTHA). Serum FFAs, insulin and glucose concentrations were measured at 0, 10, and 30 min after the [^{11}C]-palmitate injection, and 0, 30, 60, and 90 min after the [^{18}F]-FTHA injection.

TABLE 2
Characteristics of MS group according to International Diabetes Federation criteria

	Metabolic syndrome
n (female/male)	23 (15/8)
Increased waist circumference (women ≥80 cm, men ≥94 cm)	23 (15/8)
Raised triglycerides (>150.6 mg/dl)	4 (2/2)
Lowered HDL cholesterol (women <49.9 mg/dl; men <39.8 mg/dl)	7 (5/2)
Raised systolic blood pressure (>130 mmHg)	14 (10/4)
Raised diastolic blood pressure (>85 mmHg)	15 (11/4)
Raised fasting plasma glucose (≥100.8 mg/dl)	18 (12/6)

TABLE 3
Percentage distribution of brain [^{13}C]-palmitate and [^{18}F]-FTHA uptake in vivo

Radioactivity distribution from total lipids + Aq*	[^{13}C]-palmitate	[^{18}F]-FTHA	Paired Student *t* test
Aq* %	37.7 ± 0.0†	30.9 ± 9.7	NS
All lipids %	62.3 ± 0.0	69.1 ± 9.7	NS
Triglycerides %	0.6 ± 0.2	53.4 ± 11.3	$P = 0.0001$
Fatty acids %	2.2 ± 0.1	6.3 ± 3.3	NS
Phospholipids %	59.4 ± 0.3	9.4 ± 3.2	$P < 0.0001$

Number of pigs ([^{18}F]-FTHA $n = 8$, [^{13}C]-palmitate $n = 6$). *Hydrophilic phase. †The hydrophilic phase of [^{13}C]-palmitate is estimated based on tracer brain distribution curve at 3-h time point, published by Miller et al. (11). NS, not significant.

Image acquisition, processing, and corrections. Most studies were performed using GE Discovery PET-CT STE (GE, Medical Systems, Milwaukee, WI), but because of the short half-life of [^{11}C]-palmitate, Siemens ECAT HR+ (Knoxville, TN) and GE Advance (GE Medical Systems, Milwaukee, WI) were in use when this tracer was divided. The second study was scanned with same camera-protocol as the first study. Data were corrected for dead-time, decay, and photon attenuation. PET images were reconstructed in GE Advance using a 128 × 128 matrix with a 30-cm field of view (FOV) in three-dimensional (3D) mode and Filtered Back Projection (FBP) reconstruction, in Siemens HR+ using 128 × 128 matrix with zoom two (28.8 cm FOV) in 3D mode and FBP reconstruction and in PET-CT using 128 × 128 matrix with 35 cm FOV in 3D mode and Iterative Ordered Subset Expectation Maximization (OSEM) reconstruction (VUEPoint).

Calculation of the parametric fractional uptake rate image. Brain fractional uptake indexes for [^{11}C]-palmitate and [^{18}F]-FTHA were calculated by dividing the brain radioactivity by the integral of the plasma unmetabolized radioactivity curve at 15 min. The modeling gives results that are independent of the injected tracer dose. The fractional uptake rate (FUR) image from dynamic brain scanning was calculated from 10–20 min.

Analysis of PET images. The detailed description of regional and voxel level PET image analyses and statistical analyses of regional FUR estimates are provided in the online appendix. All values are expressed as mean ± SD. *P* values < 0.05 are considered statistically significant.

Biochemical analyses. Details of biochemical analyses are provided in the online appendix.

Statistical analysis of biochemical and anthropometric data. Student *t* test was used in baseline to compare results between MS patients and the control group. A paired Student *t* test was used to compare changes in the MS group before and after VLCD. Correlations were analyzed using SAS Enterprise Guide 4.1 (4.1.0.471; SAS Institute, Cary, NC). The normality of variables was assessed by the Shapiro-Wilkins test. Variables with normal distribution were calculated using Pearson correlation, and non-normal Spearman correlation was used. All values are expressed as mean ± SD. *P* values < 0.05 are considered statistically significant.

RESULTS

Metabolic characteristics during the study. Compared with the healthy control subjects, patients with MS had higher fasting plasma glucose concentrations (Table 1), but otherwise no significant differences in oral glucose tolerance test (OGTT) results between healthy control patients and MS patients were found. After VLCD, subjects with MS lost weight ~11.1 kg (range 7.2–15.4 kg, $P <$ 0.0001), whereas total cholesterol ($P < 0.0001$), LDL ($P <$

TABLE 4
Anthropometric and metabolic characteristics after VLCD

	Before VLCD	After VLCD	*P* value
Weight, kg	100.4 ± 11.7	89.4 ± 11.1	<0.0001
BMI, kg/m^2	34.0 ± 3.9	30.2 ± 3.9	<0.0001
Fasting glucose, mg/dl	180.0 ± 10.8	102.6 ± 9.0	0.02
OGTT glucose, 60 min, mg/dl	138.6 ± 39.6	117.0 ± 36.0	NS
OGTT glucose, 120 min, mg/dl	111.6 ± 27.0	104.4 ± 23.4	NS
Fasting insulin, mU/l	6.8 ± 2.6	4.6 ± 2.2	<0.0001
Total cholesterol, mg/dl	189.5 ± 30.9	143.1 ± 23.2	<0.0001
HDL cholesterol, mg/dl	50.3 ± 11.6	50.3 ± 7.7	NS
Triglycerides, mg/dl	106.3 ± 44.3	79.7 ± 26.6	<0.002
LDL cholesterol, mg/dl	116.0 ± 30.9	81.2 ± 19.3	<0.0001
HOMA index†	1.8 ± 0.7	1.2 ± 0.7	<0.0002
Free fatty acids, mmol/l	0.61 ± 0.17	0.56 ± 0.14	NS

Data are mean ± SD. Number of subjects = 16 (11 females and 5 males). †HOMA index calculated (fasting insulin × fasting glucose)/22.5; fasting insulin values are from PET-scanning day. *P* values obtained from paired Student *t* test. NS, not significant; VLCD, very low calorie diet.

0.0001), and triglycerides ($P < 0.002$) also improved (Table 4). Changes in fasting plasma glucose concentration and in fasting insulin after VLCD were significant. The percentage decrease in fasting insulin was 37.4%.

Brain fatty acid tracer accumulation over time. After injection, [^{18}F]-FTHA radioactivity in the brain increased over time (Fig. 1*A*). As shown previously, plasma [^{18}F]-FTHA and [^{11}C]-palmitate concentration decreased quickly after injection (9,19,20). The increase in tissue radioactivity over time with [^{18}F]-FTHA reflects label trapping (Fig. 1). As shown in an example of brain image after [^{18}F]-FTHA injection (Fig. 2), radioactivity was highest in the thalamus (the two largest gray matter nuclei in the center of the transaxial image), followed by high uptake in the basal ganglia and throughout the cerebral cortex.

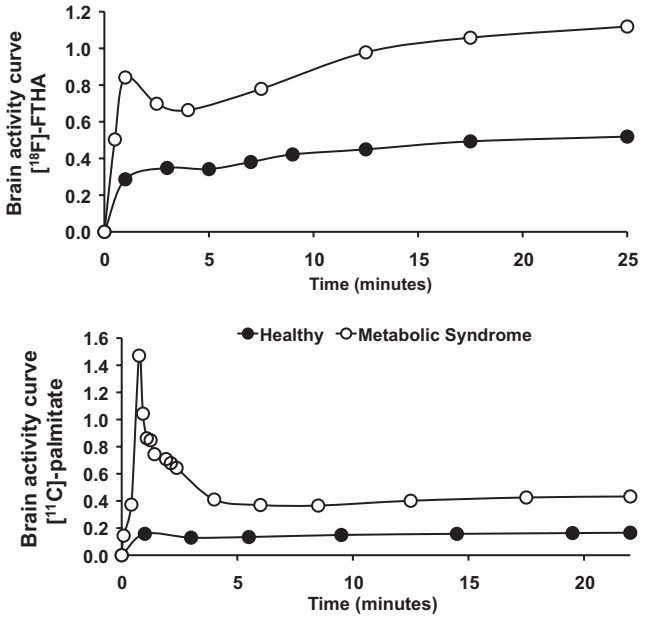

FIG. 1. An example of a time course of brain tissue radioactivity after intravenous injection of [^{18}F]-FTHA and [^{11}C]-palmitate from one nonobese healthy subject and one obese subject with MS. The values are given as standardized uptake values (SUVs), and values are normalized to the dosage (MBq), and body weight (kg). The resulting SUV value has been multiplied with individual blood FFA level. The increase in brain radioactivity over time with [^{18}F]-FTHA reflects tracer trapping. Black circles, healthy; white circles, MS.

Brain FFA uptake in healthy subjects and patients with MS. When brain FFA uptake was measured using [^{18}F]-FTHA and the values of plasma FFA concentration during PET, the brain FFA uptake was significantly higher in patients with MS compared with healthy subjects (Fig. 2). The mean percentage increase was +130% in the white matter and +47% in the gray matter, and respective standardized effect sizes were 1.83 and 0.88. The main effect of the group was significant in the repeated measures ANOVA (rmANOVA) ($F = 7.38$, $P = 0.012$), whereas no effect from the scanner was observed. In addition, the group × region interaction was significant ($F = 5.35$, $P = 0.016$), indicating that the group difference in [^{18}F]-FTHA uptake was not uniform across brain regions. Regional ANOVAs indicated significant group differences in all regions: white matter ($P = 0.001$), anterior cingulate ($P = 0.038$), parietal ($P = 0.015$), temporal ($P = 0.015$) and prefrontal cortex ($P = 0.020$), amygdala-hippocampal complex ($P = 0.014$), striatum ($P = 0.019$), and hypothalamus ($P = 0.007$). The mean percentage increment in the hypothalamic area was +52% among the subjects with MS compared with healthy subjects. No scanner effects were seen in any region. A marked elevation was also found in the brain uptake of [^{11}C]-palmitate in patients with MS when compared with healthy controls (Fig. 2). The average increase was +83.8% in the white matter and +87.7% in the gray matter. The standardized effect sizes were of large magnitude, 1.24 in both the white and gray matter. The rmANOVA also demonstrated a significant main effect of group ($P = 0.017$). Because different PET-scanners were used in this study, we wanted to test whether the use of different PET-scanners would have an impact on the findings. The rmANOVA demonstrated no effects of the scanner ($P = 0.959$). The group × region interaction was also significant ($P = 0.016$), suggesting that elevation of [^{11}C]-palmitate uptake in the brain in patients with MS might vary across brain regions. In ANOVA models, predicting regional [^{11}C]-palmitate uptake with group status and scanner demonstrated significant group differences in all brain regions: white matter ($P = 0.021$), anterior cingulate ($P = 0.028$), parietal ($P = 0.011$), temporal ($P = 0.013$) and prefrontal cortex ($P = 0.015$), amygdala-hippocampal complex ($P = 0.016$), striatum ($P = 0.029$) and hypothalamus ($P = 0.016$). The mean percentage change in hypothalamic area was +88% among the subjects with MS compared with healthy subjects. The uptake of [^{18}F]-FTHA correlated positively with [^{11}C]-palmitate in all analyzed brain areas, and all the correlations were statistically significant. For the hypothalamus, the correlation *r* value was 0.58 ($P = 0.003$).

The effect of dieting on brain FFA uptake. There was a substantial reduction in the brain uptake of [^{18}F]-FTHA in patients with MS after VLCD (Fig. 3). The mean percentage decrease was −17.5% in the white matter and −17.6% in the gray matter. In the rmANOVA, the main effect of repetition was statistically significant ($P = 0.010$), whereas the repetition × region interaction was not ($P = 0.099$). The latter suggests that the decrease in tracer uptake was

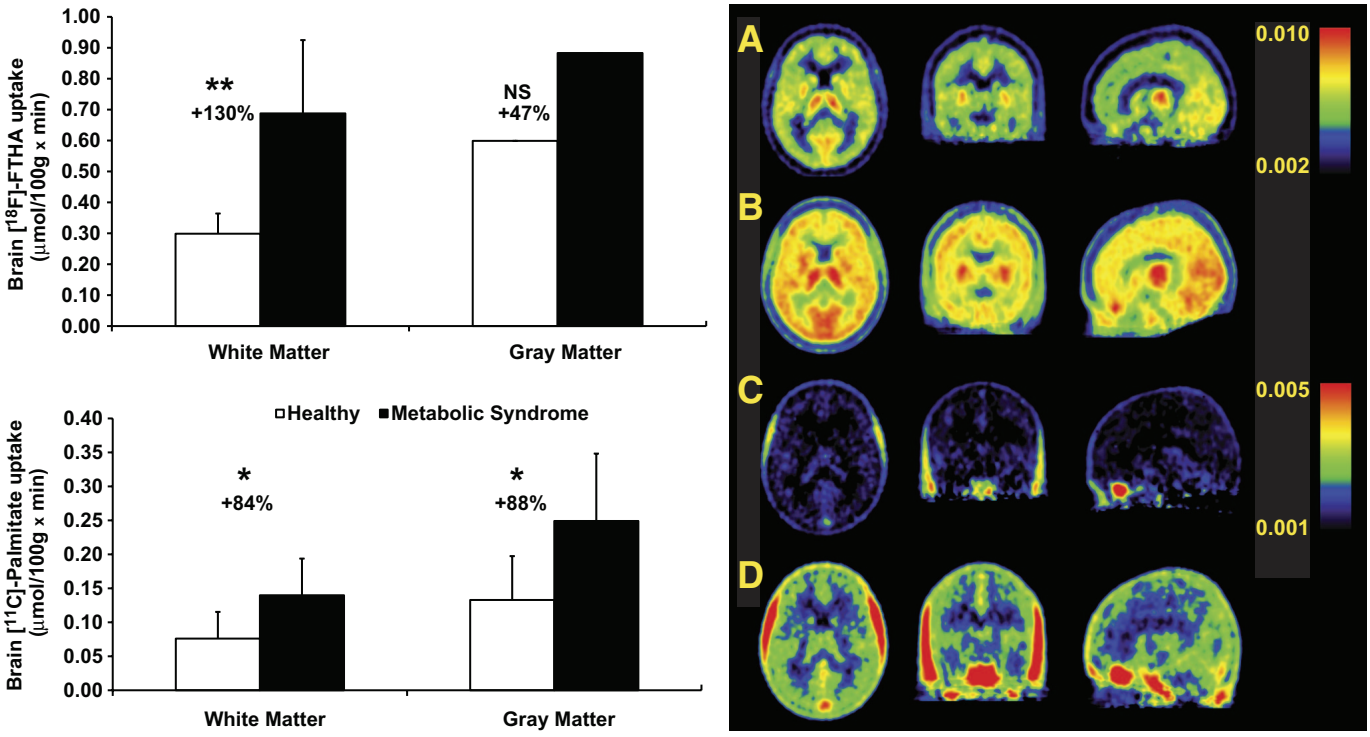

FIG. 2. ***Left*: Baseline brain white and gray matter uptake rates of [^{18}F]-FTHA (*A*) and [^{11}C]-palmitate (*B*). *P* values were calculated using Student *t* test. **P* value of 0.01; ***P* value of 0.0006. NS, not significant. White bars, healthy; black bars, MS. *Right*: Transaxial, coronal, and sagittal sections of group-wise [^{18}F]-FTHA-PET and [^{11}C]-palmitate-PET images of the brain in healthy controls (*A* and *C*) and MS patients (*B* and *D*). *A*: [^{18}F]-FTHA-PET healthy control. *B*: [^{18}F]-FTHA PET MS. *C*: [^{11}C]-palmitate-PET healthy control. *D*: [^{11}C]-palmitate-PET MS. Images represent average spatially normalized uptake images, and the scale is mmol/(100g × min). In the PET images, the highest activity is shown in red as an index of tracer accumulation. The difference between [^{18}F]-FTHA and [^{11}C]-palmitate is that [^{18}F]-FTHA is metabolically trapped whereas [^{11}C]-palmitate is not. Higher activity of [^{18}F]-FTHA reflects the accumulation of the tracer in the brain tissue. (A high-quality digital representation of this figure is available in the online issue.)**

uniform across brain regions. Therefore, to avoid type 1 errors, regional changes were not formally assessed. This result was confirmed using a voxel-based mapping analysis (Fig. 3). The change in [^{11}C]-palmitate uptake was highly variable between individuals, with the average across regions ranging from −37% to +210% and the average across individuals being +32% (SD 74%). The rmANOVA did not show any significant change in [^{11}C]-palmitate uptake after VLCD (Fig. 3, main effect of repetition: $P = 0.712$, repetition × region interaction: $P = 0.676$). The change in [^{18}F]-FTHA uptake versus change in [^{11}C]-palmitate correlated positively in all brain areas, and all of the correlations were statistically significant. For the hypothalamus, the correlation r value was 0.56 ($P < 0.05$).

Fatty acid uptake and metabolic characteristics. Brain fatty acid uptake measured with [^{18}F]-FTHA-PET was positively associated with age ($P = 0.007$, $r = 0.52$), fasting serum insulin ($P < 0.05$, $r = 0.40$) and homeostasis model assessment (HOMA) index ($P = 0.04$, $r = 0.41$) (Fig. 4). The correlation between [^{18}F]-FTHA and age persisted after the data were adjusted for BMI ($P < 0.03$, $r = 0.46$). Both total and nonoxidized fraction of fatty acid uptake were positively associated with the BMI (total: $P = 0.002$, nonoxidized: $P = 0.004$).

DISCUSSION

To our knowledge, this is the first study to investigate brain FFA uptake in obese patients with MS. The main finding of the study is that patients with MS have higher FFA uptake in the brain compared with healthy subjects. Weight loss reduced FFA uptake more in healthy subjects, and this was more due to decreased FFA oxidation rather than decreased metabolic FFA utilization.

We and others have previously used [^{18}F]-FTHA and PET to quantify regional FFA metabolism, especially in myocardium and skeletal muscle (18,20,21). Recently we showed that [^{18}F]-FTHA accumulates in the brain in significant amounts (18), thus making it a reliable tracer to quantify brain FFA uptake. The brain tissue-input ratio for [^{18}F]-FTHA ratio was high, suggesting that [^{18}F]-FTHA crosses the blood-brain barrier and accumulates persistently and in measurable amounts. More than half of the tracer was going into the lipids, and less than half into the breakdown products (18). These breakdown products likely represent oxidation, so the study results suggest that [^{18}F]-FTHA reflects total uptake. [^{11}C]-palmitate has been shown to accumulate in monkey brain (9) and the extracted fraction is independent of cerebral flow (22). Palmitate accumulation in the brain has also been verified in rats (11,23–25), and the flux is proportional to published values for regional brain oxidative metabolism (23). Long-chain saturated fatty acids such as [^{11}C]-palmitate enter, to a large extent (50–60%), via β-oxidation in mitochondria, creating radioactive, aqueous metabolites, particularly glutamate, glutamine, and aspartate, whereas the other half is incorporated into lipids (22,26,27). After the fast oxidation of [^{11}C]-palmitate, the remaining radioactivity thus enters the stable lipid pool of the brain representing nonoxidative residual. It has been suggested that 83% of brain radioactivity is in stable compartments within 2 min after a steady-state level of plasma palmitate is achieved (9). Plasma [^{11}C]-palmitate activity in our study was stable

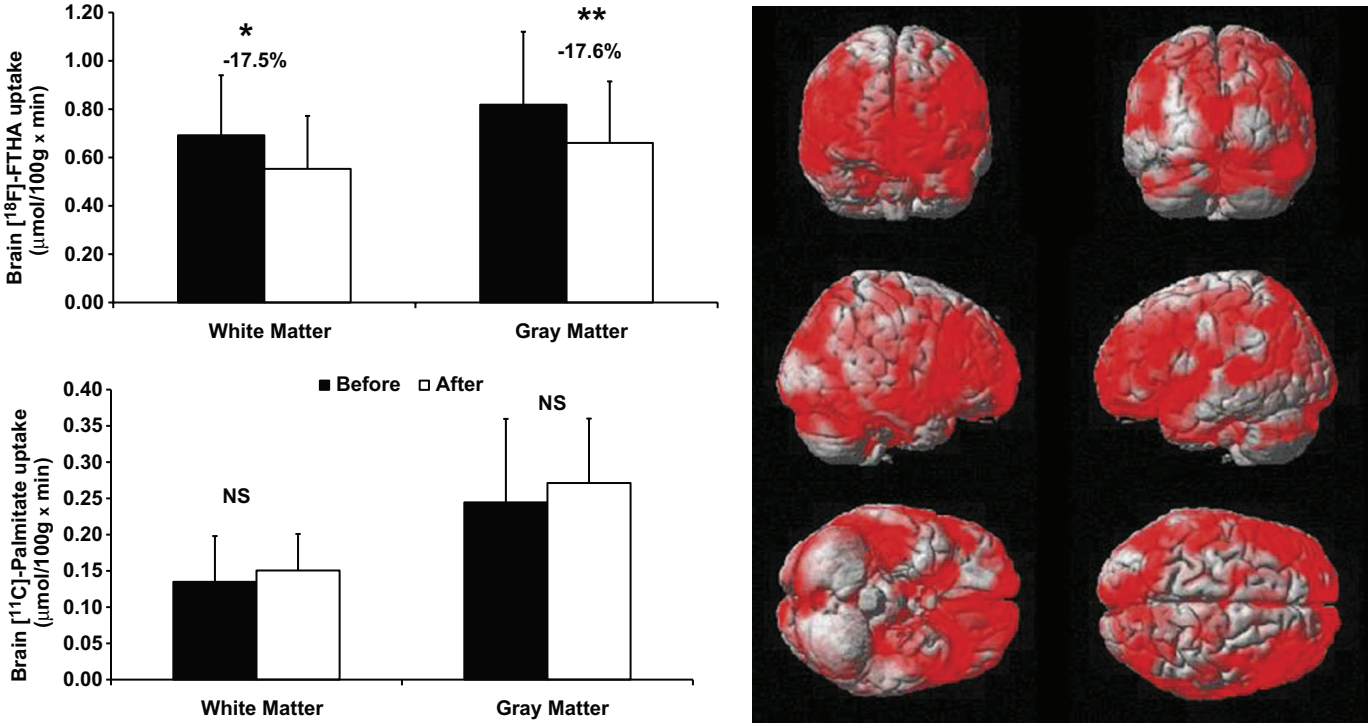

FIG. 3. ***Left*****: Graphs show the results of brain white and gray matter uptake of [^{18}F]-FTHA and [^{11}C]-palmitate in the MS group before and after VLCD.** ***P*** **values were calculated using paired Student** ***t*** **test. ****P* **value < 0.02; *****P* **value of 0.009; NS, not significant; black bars, before VLCD; white bars, after VLCD.** ***Right*****: Results from the voxel-based mapping analysis. Results are rendered on an anatomical brain model; red areas illustrate brain regions where [^{18}F]-FTHA uptake was significantly reduced after dieting among MS patients (T_{max} = 4.21 at (−66, −22, 48), kE = 161,315, cluster-level corrected** ***P*** **< 0.0005). (A high-quality digital representation of this figure is available in the online issue.)**

shortly after 5 min in each person. Because the analysis was done using time frames of 10–20 min, the palmitate results from brain can be considered to represent incorporation to stable compartments, and thus the so-called nonoxidative residual. We speculate that by combining the information from [^{18}F]-FTHA and [^{11}C]-palmitate, it may be possible to estimate the brain FFA oxidative component as the difference between total and nonoxidative fatty acid uptake ([^{18}F]-FTHA minus [^{11}C]-palmitate). From our in vivo validation study, we found that both [^{13}C]-palmitate and [^{18}F]-FTHA are incorporated into the brain in measurable amounts. The percentage found in the brain hydrophilic and lipid pool did not differ between tracers, whereas a difference was seen in distribution within the lipid pool. From both tracers, we found that more than 60% were found in the lipid pool; [^{18}F]-FTHA was mainly in triglycerides, whereas [^{13}C]-palmitate was mainly recovered from phospholipids. The conversion of [^{18}F]-FTHA to phospholipids might be different because of steric or charge hindrance. However, the in vivo validation was to show that both tracers are stored in the brain in similar amounts. The distribution of tracers within lipid pool itself is not addressed since PET cannot distinguish between these storage forms.

The brain uptake of [^{18}F]-FTHA and [^{11}C]-palmitate was increased in patients with MS compared with healthy individuals. The difference with [^{18}F]-FTHA was not uniformly increased in all brain areas. The total FFA uptake was significantly greater in the white matter among subjects with MS compared with healthy controls, and the increment appeared to be of larger magnitude than that in the gray matter. The increase in white matter [^{18}F]-FTHA uptake could contribute to previous findings of brain white matter expansion among obese subjects (28). The differ-

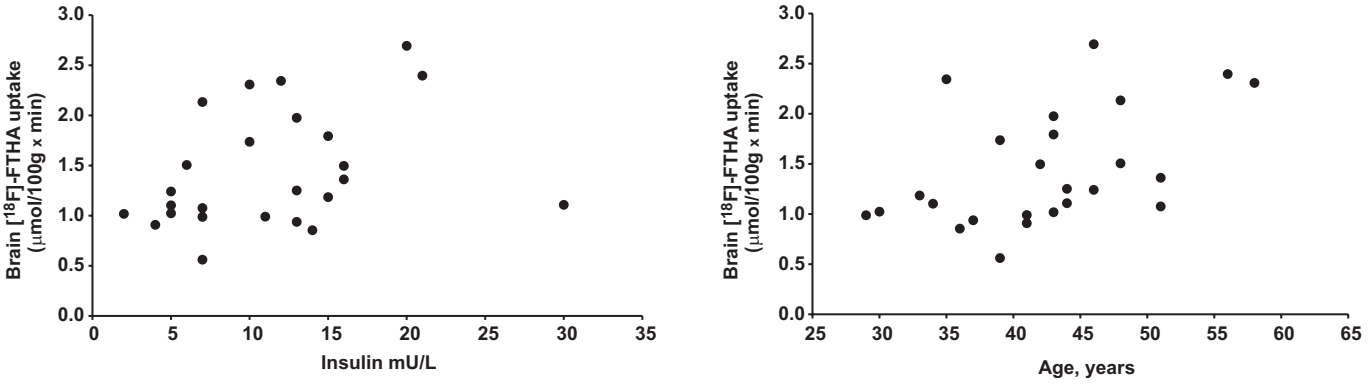

FIG. 4. The brain uptake of [^{18}F]-FTHA representing total brain FFA uptake positively correlated with fasting insulin (*P* < 0.05; *r* = 0.40) and age (*P* = 0.007; *r* = 0.52). Fasting insulin values are taken from OGTT.

ence with [^{11}C]-palmitate between groups was more uniform and thus statistically significant in all analyzed areas. The hypothalamic area, now associated with fatty acid sensing and regulation of energy balance and feeding (2,4), had also increased uptake of both [^{11}C]-palmitate and [^{18}F]-FTHA. Weight loss reduced the [^{18}F]-FTHA uptake uniformly in all brain regions, including the hypothalamus. It is hypothesized that reduced [^{18}F]-FTHA uptake simultaneously with no change in [^{11}C]-palmitate uptake might reflect reduction in brain FFA oxidative component. This result is in line with a recent rodent study in which inhibition of hypothalamic β-oxidation normalized the energy homeostasis of the animals (5). Thus, the changes in the oxidative component seem to be related more to weight control and satiety, supporting our finding that oxidative metabolism is different in the obese MS group and could be partially reversed by weight loss. There was no statistically significant difference in nonoxidative storage component after weight loss, but the change in [^{11}C]-palmitate uptake was highly variable between individuals. The reason why a decrease was seen in [^{18}F]-FTHA uptake but not in [^{11}C]-palmitate could be that oxidative metabolism might be more flexible in nature, whereas the synthesis of complex lipids may be more preserved due to its important structural role in the brain. In addition, these studies were conducted under fasting conditions, which are characterized by activation of FFA oxidative metabolism. This may also help explain why intervention-related differences in this process are more easily identified than those in storage. The dieting period did not affect fasting plasma FFA levels, thus multiplying image data with individual FFA level does not contribute to the observed decrease in FFA uptake.

Our findings are consistent with recent studies implicating the role of hypothalamic fatty acid sensing and their role in the regulation of feeding, energy balance (2,4,5), and peripheral physiologic processes (29). The normalization of hypothalamic lipid sensing has been linked to normalization of energy and glucose homeostasis (5). From our study results, it seems that the normal catabolic effect of central FFAs is disturbed in obesity, and this is at least partially reversible after weight loss. Peripheral insulin resistance contributing to MS could also affect the brain. In healthy pigs, hyperinsulinemia induced ~20–50% decrease in brain [^{18}F]-FTHA radioactivity compared with fasting state (18). The hypothesized central insulin resistance could interfere with brain glucose utilization, thus resulting in compensatory increased FFA uptake and FFA oxidation. Weight loss is known to improve insulin sensitivity and plasma lipid profile (30). The beneficial effect of weight loss was observed in our study among MS patients; in addition to beneficial peripheral effects, FFA uptake in the brain was uniformly decreased due to a decrease in FFA oxidation. The correlations from our study corroborate this line of interference: FFA uptake was positively correlated with BMI, plasma insulin, and HOMA-index; among these, BMI had the strongest correlation. Brain FFA uptake also increased with ageing, suggesting that ageing is related to degenerative changes in the metabolic processes, and reinforcing the theory that age is a risk factor for MS.

Given that the activation of hypothalamic nuclei can result in changes in sympathetic tone, and that hypothalamus is a key regulator in feeding and energy balance, it is interesting to hypothesize that central FFAs could contribute to increased sympathetic tone in obesity. Previous studies support both positive and negative effects of central lipids in sympathetic tone. It has been reported that central lipid infusion resulting in increased brain lipids might modulate sympathoadrenal response (31), and that intracerebrovascular infusion of fatty acids might lower sympathetic activity. Unfortunately, we did not have any direct measurements to address this question.

Limitations in this study were the small number of subjects in the healthy control group and the fact that all of the healthy subjects were males. If sex is used in the statistical model as a covariate, the group difference in [^{18}F]-FTHA uptake persists in the white matter (group × region: $F = 6.72$, $P = 0.007$; main effect of group in the white matter: $F = 4.92$, $P = 0.037$), but not in other brain regions, and no significant effects are seen with [^{18}F]-palmitate. In addition, female patients with MS had higher uptake values for both radioligands than male patients with MS. Future studies including healthy females should establish whether a significant interaction exists between sex and disease status, such that female patients may be more severely affected than male patients, as current data suggest. However, we think that a simple confounding main effect of sex is unlikely to explain the current results, based on three facts. First, [^{18}F]-FTHA uptake is increased in MS in white matter even when sex is taken into account. Second, significant correlations were seen between fatty acid uptake and clinical variables, such as BMI and fasting plasma glucose, suggesting that increased fatty acid uptake is more likely related to metabolic abnormalities than sex alone. Third, the significant decrease in fatty acid uptake after weight loss argues against a main effect of sex because such main effect would not be reversible. Nevertheless, we acknowledge the skewed sex distribution as a limitation to the interpretation of the results, and recommend that sex be taken into account in future studies. The number of subjects having MS differs in cross-section versus VLCD intervention. The first phase of the study was only cross-sectional. After having positive results from phase 1, we wanted to study in more detail the possibility that brain FFA uptake is related to weight. The more comprehensive phase two (VLCD intervention) was introduced in the study protocol and the last 16 of 23 subjects took part in this phase. Another limiting factor is that the brain kinetics of [^{18}F]-FTHA is not known so well as in other organs and was assumed to be taken up as natural palmitate. Although the in vivo biodistribution of [^{18}F]-FTHA in the brain suggests that [^{18}F]-FTHA represents total uptake, it does not prove that it equals uptake of natural FFAs. In our study, the total oxidation of [^{11}C]-palmitate was found to be less than 50%. In the animal studies, it has been found that approximately 60% of the [^{11}C]-palmitate enters to β-oxidation (9). It is possible that the kinetic properties of [^{18}F]-FTHA differ slightly from our assumption, explaining the slight difference between our study and animal studies. Nevertheless, this would not affect the differences found between the two groups. The dosages of injected tracers did not explain the findings, even when weight was taken into account. In addition, the isocaloric diet was not controlled, but the subjects were free to eat what they wanted. So the quality and quantity of the foods probably differ between subjects.

To conclude, we have found that patients fulfilling the International Diabetes Federation criteria of metabolic syndrome have increased brain FFA uptake when compared with healthy subjects. Weight loss is able to partly reverse this abnormality. These novel findings highlight

the possible role of brain FFAs in regulation of body weight. It seems that the normal catabolic effect of central FFAs is disturbed in MS and this is partially reversed after weight loss.

ACKNOWLEDGMENTS

The study was conducted in the Finnish Centre of Excellence in Molecular Imaging in Cardiovascular and Metabolic Research, supported by the Academy of Finland, University of Turku, Turku University Hospital, and Åbo Academy University. Support was also received by grants from the HEPADIP EU FP6 program, the Novo Nordisk Foundation, and the Hertta and Veikko Valtonen Foundation.

No other potential conflicts of interest relevant to this article were reported.

A.K. wrote the manuscript, researched data, contributed to discussion, and reviewed/edited the manuscript. P.I. and P.N. contributed to discussion and reviewed/edited the manuscript. A.V., K.V., V.O. J.K., T.V., L.G., and M.H.-S. researched data. J.H. researched data, wrote the manuscript, and reviewed/edited the manuscript. B.A.F. researched data and contributed to discussion. K.N. reviewed the manuscript. O.S. researched data and reviewed the manuscript.

REFERENCES

1. Obici S, Feng Z, Morgan K, Stein D, Karkanias G, Rossetti L. Central administration of oleic acid inhibits glucose production and food intake. Diabetes 2002;51:271–275
2. Lopez M, Lelliott CJ, Vidal-Puig A. Hypothalamic fatty acid metabolism: a housekeeping pathway that regulates food intake. Bioessays 2007;29:248–261
3. Lopez M, Lage R, Saha AK, Perez-Tilve D, Vazquez MJ, Varela L, Sangiao-Alvarellos S, Tovar S, Raghay K, Rodriguez-Cuenca S, Deoliveira RM, Castaneda T, Datta R, Dong JZ, Culler M, Sleeman MW, Alvarez CV, Gallego R, Lelliott CJ, Carling D, Tschop MH, Dieguez C, Vidal-Puig A. Hypothalamic fatty acid metabolism mediates the orexigenic action of ghrelin. Cell Metab 2008;7:389–399
4. Lam TK, Schwartz GJ, Rossetti L. Hypothalamic sensing of fatty acids. Nat Neurosci 2005;8:579–584
5. Pocai A, Lam TK, Obici S, Gutierrez-Juarez R, Muse ED, Arduini A, Rossetti L. Restoration of hypothalamic lipid sensing normalizes energy and glucose homeostasis in overfed rats. J Clin Invest 2006;116:1081–1091
6. Miranda PJ, DeFronzo RA, Califf RM, Guyton JR. Metabolic syndrome: definition, pathophysiology, and mechanisms. Am Heart J 2005;149:33–45
7. Eckel RH, Grundy SM, Zimmet PZ. The metabolic syndrome. Lancet 2005;365:1415–1428
8. Morgan K, Obici S, Rossetti L. Hypothalamic responses to long-chain fatty acids are nutritionally regulated. J Biol Chem 2004;279:31139–31148
9. Arai T, Wakabayashi S, Channing MA, Dunn BB, Der MG, Bell JM, Herscovitch P, Eckelman WC, Rapoport SI, Chang MC. Incorporation of [1-carbon-11]palmitate in monkey brain using PET. J Nucl Med 1995;36:2261–2267
10. Kimes AS, Sweeney D, Rapoport SI. Brain palmitate incorporation in awake and anesthetized rats. Brain Res 1985;341:164–170
11. Miller JC, Gnaedinger JM, Rapoport SI. Utilization of plasma fatty acid in rat brain: distribution of [14C]palmitate between oxidative and synthetic pathways. J Neurochem 1987;49:1507–1514
12. Tabata H, Kimes AS, Robinson PJ, Rapoport SI. Stability of brain incorporation of plasma palmitate in unanesthetized rats of different ages, with appendix on palmitate model. Exp Neurol 1988;102:221–229
13. Knuuti J. Positron emission tomography–molecular imaging of biological processes. International Congress Series 2004;1265:248–254
14. Alberti KG, Zimmet P, Shaw J. The metabolic syndrome—a new worldwide definition. Lancet 2005;366:1059–1062
15. Padgett HC, Robinson GD, Barrio JR. [1-(11)C]palmitic acid: improved radiopharmaceutical preparation. Int J Appl Radiat Isot 1982;33:1471–1472
16. DeGrado TR, Coenen HH, Stocklin G. 14(R,S)-[18F]fluoro-6-thia-heptadecanoic acid (FTHA): evaluation in mouse of a new probe of myocardial utilization of long chain fatty acids. J Nucl Med 1991;32:1888–1896
17. DeGrado TR, Wang S, Holden JE, Nickles RJ, Taylor M, Stone CK. Synthesis and preliminary evaluation of (18)F-labeled 4-thia palmitate as a PET tracer of myocardial fatty acid oxidation. Nucl Med Biol 2000;27:221–231
18. Guiducci L, Gronroos T, Jarvisalo MJ, Kiss J, Viljanen A, Naum AG, Viljanen T, Savunen T, Knuuti J, Ferrannini E, Salvadori PA, Nuutila P, Iozzo P. Biodistribution of the fatty acid analogue 18F-FTHA: plasma and tissue partitioning between lipid pools during fasting and hyperinsulinemia. J Nucl Med 2007;48:455–462
19. Ebert A, Herzog H, Stocklin GL, Henrich MM, DeGrado TR, Coenen HH, Feinendegen LE. Kinetics of 14(R,S)-fluorine-18-fluoro-6-thia-heptadecanoic acid in normal human hearts at rest, during exercise and after dipyridamole injection. J Nucl Med 1994;35:51–56
20. Iozzo P, Turpeinen AK, Takala T, Oikonen V, Solin O, Ferrannini E, Nuutila P, Knuuti J. Liver uptake of free fatty acids in vivo in humans as determined with 14(R, S)-[18F]fluoro-6-thia-heptadecanoic acid and PET. Eur J Nucl Med Mol Imaging 2003;30:1160–1164
21. Takala TO, Nuutila P, Pulkki K, Oikonen V, Gronroos T, Savunen T, Vahasilta T, Luotolahti M, Kallajoki M, Bergman J, Forsback S, Knuuti J. 14(R,S)-[18F]Fluoro-6-thia-heptadecanoic acid as a tracer of free fatty acid uptake and oxidation in myocardium and skeletal muscle. Eur J Nucl Med Mol Imaging 2002;29:1617–1622
22. Robinson PJ, Noronha J, DeGeorge JJ, Freed LM, Nariai T, Rapoport SI. A quantitative method for measuring regional in vivo fatty-acid incorporation into and turnover within brain phospholipids: review and critical analysis. Brain Res Brain Res Rev 1992;17:187–214
23. Kimes AS, Sweeney D, London ED, Rapoport SI. Palmitate incorporation into different brain regions in the awake rat. Brain Res 1983;274:291–301
24. Gnaedinger JM, Miller JC, Latker CH, Rapoport SI. Cerebral metabolism of plasma [14C]palmitate in awake, adult rat: subcellular localization. Neurochem Res 1988;13:21–29
25. Robinson PJ, Rapoport SI. A method for examining turnover and synthesis of palmitate-containing brain lipids in vivo. Clin Exp Pharmacol Physiol 1989;16:701–714
26. Chang MC, Wakabayashi S, Bell JM. The effect of methyl palmoxirate on incorporation of [U-14C]palmitate into rat brain. Neurochem Res 1994;19:1217–1223
27. Chang MC, Grange E, Rabin O, Bell JM. Incorporation of [U-14C]palmitate into rat brain: effect of an inhibitor of beta-oxidation. J Lipid Res 1997;38:295–300
28. Haltia LT, Viljanen A, Parkkola R, Kemppainen N, Rinne JO, Nuutila P, Kaasinen V. Brain white matter expansion in human obesity and the recovering effect of dieting. J Clin Endocrinol Metab 2007;92:3278–3284
29. Pocai A, Obici S, Schwartz GJ, Rossetti L. A brain-liver circuit regulates glucose homeostasis. Cell Metab 2005;1:53–61
30. Shadid S, LaForge R, Otvos JD, Jensen MD. Treatment of obesity with diet/exercise versus pioglitazone has distinct effects on lipoprotein particle size. Atherosclerosis 2006;188:370–376
31. Haywood SC, Bree AJ, Puente E, Daphna-Iken D, Fisher SJ. Central, but not systemic lipid infusion, augments the counterregulatory response to hypoglycemia. Am J Physiol Endocrinol Metab 2009;297:E50–E56